



OPEN

Endothelial inflammation and neutrophil transmigration are modulated by extracellular matrix composition in an inflammation-on-a-chip model

Rebecca B. Riddle¹, Karin Jennbacken², Kenny M. Hansson² & Matthew T. Harper¹✉

Inflammatory diseases are often characterised by excessive neutrophil infiltration from the blood stream to the site of inflammation, which damages healthy tissue and prevents resolution of inflammation. Development of anti-inflammatory drugs is hindered by lack of *in vitro* and *in vivo* models which accurately represent the disease microenvironment. In this study, we used the OrganoPlate to develop a humanized 3D *in vitro* inflammation-on-a-chip model to recapitulate neutrophil transmigration across the endothelium and subsequent migration through the extracellular matrix (ECM). Human umbilical vein endothelial cells formed confluent vessels against collagen I and geltrex mix, a mix of basement membrane extract and collagen I. TNF- α stimulation of vessels upregulated inflammatory cytokine expression and promoted neutrophil transmigration. Intriguingly, major differences were found depending on the composition of the ECM. Neutrophils transmigrated in higher number and further in geltrex mix than collagen I, and did not require an *N*-formyl-methionyl-leucyl-phenylalanine (fMLP) gradient for transmigration. Inhibition of neutrophil proteases inhibited neutrophil transmigration on geltrex mix, but not collagen I. These findings highlight the important role of the ECM in determining cell phenotype and response to inhibitors. Future work could adapt the ECM composition for individual diseases, producing accurate models for drug development.

Inflammatory responses are required to successfully combat invasion by pathogens. However, excessive or unresolved inflammation can damage healthy tissue and result in chronic inflammatory conditions such as rheumatoid arthritis, ulcerative colitis, cardiomyopathies, cardiovascular disease, and asthma.

During an inflammatory response, neutrophils move from the blood to the site of inflammation by trans-migrating across the endothelial barrier and through the basement membrane (BM) of the surrounding extra-cellular matrix (ECM). This multi-step process is enabled by inflammatory receptors and molecules expressed by the endothelial cells which capture the neutrophils and support their extravasation, alongside gradients of chemokines that guide the neutrophils through the ECM. The neutrophils respond by upregulating integrins that allow attachment to the endothelium and subsequently aid their movement through the BM¹. These events must be tightly regulated to prevent excessive inflammation and tissue damage. Conversely, neutrophil transmigration is a potential drug target for treatment of chronic inflammatory conditions. However, crucial to developing novel therapies is a clear understanding of how neutrophil transmigration is regulated.

Neutrophil transmigration *in vivo* occurs in a 3D environment, and therefore typical 2D *in vitro* techniques cannot accurately recapitulate the process^{2,3}. Static assays such as transwell migration in Boyden chambers⁴ are hindered by effects of gravity, lack of physiological flow, and difficulty in visualizing and analysing the neutrophils at each stage of transmigration. Equally, studying neutrophils using *in vivo* animal models has important ethical implications and can inaccurately model human physiology⁵. For example, in humans neutrophils comprise

¹Department of Pharmacology, University of Cambridge, Cambridge, UK. ²Bioscience Cardiovascular, Research and Early Development, Cardiovascular, Renal and Metabolism, R&D BioPharmaceuticals, AstraZeneca, Gothenburg, Sweden. ✉email: mth29@cam.ac.uk

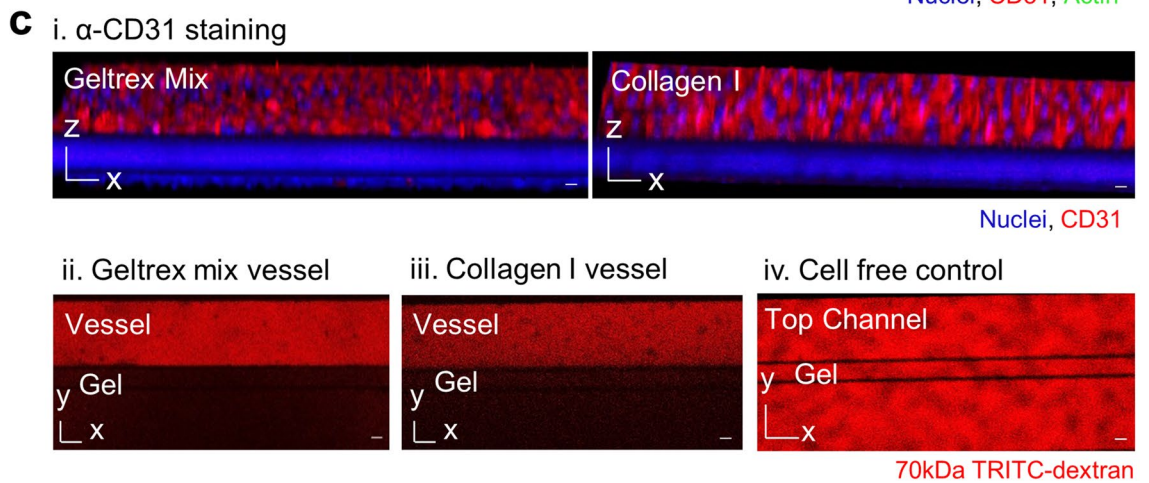
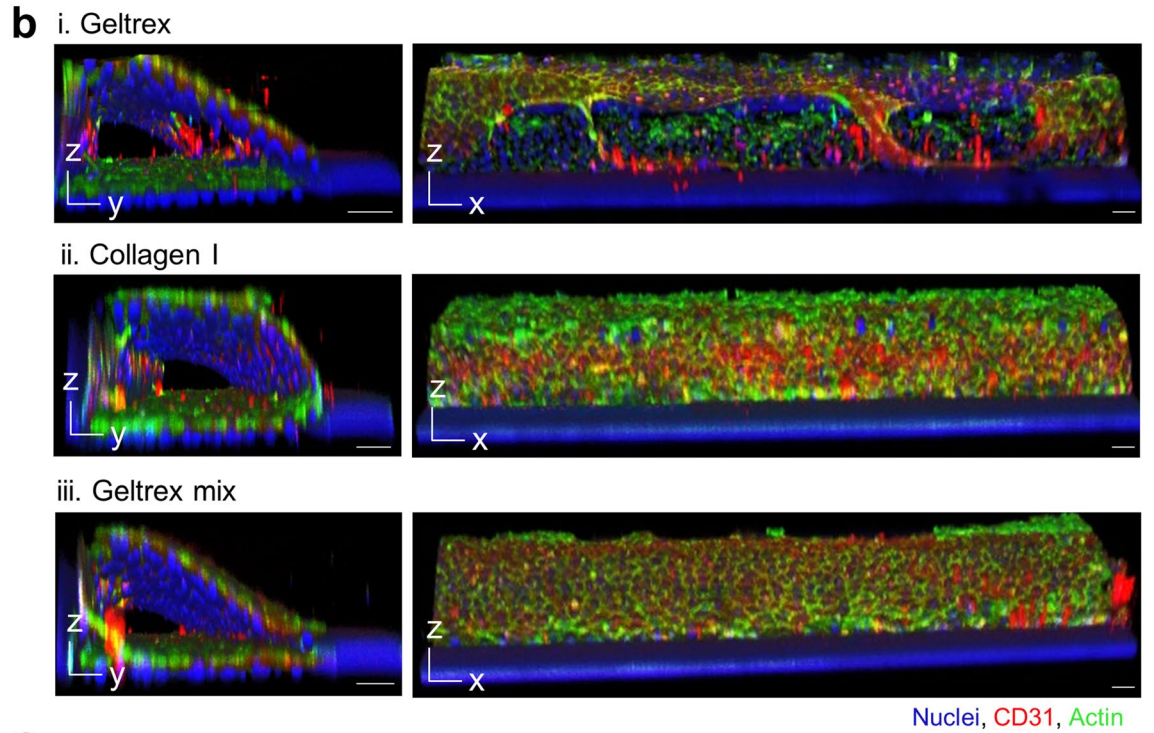
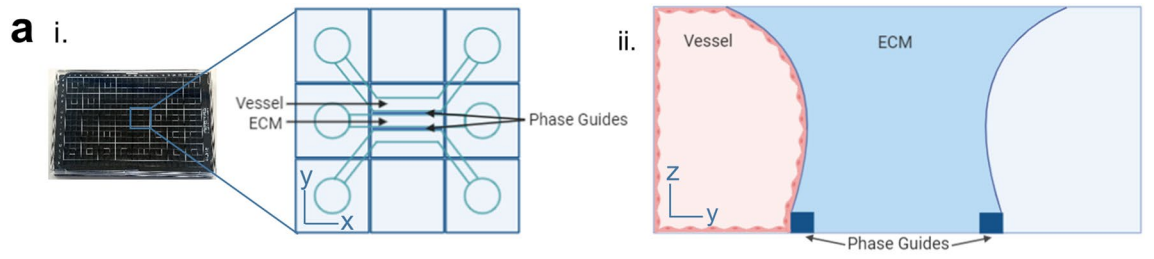


Figure 1. Incorporating collagen type I into geltrex extracellular matrix (ECM) enables formation of a leak-tight endothelial vessel in the 3-lane OrganoPlate. **(a)** 3-lane OrganoPlate schematics. i. The 3-lane OrganoPlate consists of 40 chips in a 384-well microplate format. Each chip has three lanes separated by two PhaseGuides™ which support patterning of hydrogels and cells via inlets and outlets. ii. Addition of hydrogel into the middle channel forms a barrier against which cells can be seeded in the top channel. Induction of flow via passive liquid levelling promotes vessel formation. The bottom channel is kept empty during vessel formation. **(b)** Vessel formation against different ECMs. ECM was introduced into the middle channel and incubated for 1 h to allow polymerisation. Human umbilical vein endothelial cells (HUVEC) were seeded into the top channel, left to adhere for two hours, and then placed on a plate rocker and incubated for 1 week. Vessels were fixed and then stained with Hoechst-33342 (blue), α -CD31 (red), and phalloidin-FITC (green). Images were taken on a Leica SP5 confocal microscope. 3D reconstructions of Z-stacks were produced in FIJI. Images are representative of at least $N = 3$ independent experiments. i. 14.6 mg/mL geltrex induced HUVEC tube formation against the ECM. ii. HUVEC formed confluent vessels against 4 mg/mL collagen I. iii. Incorporation of 0.75 mg/mL collagen I into 14.6 mg/mL geltrex (25:75) prevented tube formation and supported confluent vessel formation. **(c)** Vessels grown against geltrex + 25% collagen I exhibited physiological barrier function. i. HUVEC cultured in the 3-lane OrganoPlate formed intercellular junctions, as demonstrated by α -CD31 staining (red). ii. Mature vessels retained 70 kDa tetramethylrhodamine (TRITC)-dextran (red). 0.5 mg/mL TRITC-dextran was added to the vessel channel after 1 week of cell culture and incubated for 30 min. Dye retention was then imaged on a Leica SP5 confocal microscope. Scale bars are representative of 50 μ m.

50–70% of circulating leukocytes, compared to just 10–25% in mice⁶. Additionally, some cytokines found to play an important role in human inflammation such as IL-8⁷, are not expressed by mice. This lack of translation from current *in vitro* and *in vivo* models into humans has led to challenges in drug discovery⁸.

Organ-on-a-chip is a new and fast-growing field that has the potential to cross the translation gap and provide humanized models for use in both basic biology research and drug discovery. These computer chip-sized devices provide cells with a more physiological 3D environment that supports cell differentiation, enabling organ-like functions. The chips commonly consist of channels coated with ECM proteins and lined with one or more cell types. Additional physical factors such as shear flow, air–liquid interfaces, and cyclical deformation of the chips can also be incorporated^{9,10}. With developments in stem cell biology, there is potential to derive cells from induced pluripotent stem cells of patient samples, increasing the feasibility of personalised medicine¹¹. To reach this stage, models of different organs and biological processes and/or diseases need to be developed. Although the field is still relatively new, many organs have already been successfully modelled, including the lungs^{12–14}, heart^{15–17}, liver^{18,19}, kidneys²⁰, and skin^{21–23}.

To model neutrophil transmigration during inflammation, the key components are the endothelial barrier and the ECM encountered post-transmigration. Neutrophils most commonly extravasate through post-capillary venules, which increase in permeability during inflammation. To recapitulate this, inflammatory mediators such as TNF- α are used to stimulate the endothelial barrier and induce production of inflammatory molecules that promote transmigration. After crossing the endothelium, neutrophils then encounter the basement membrane, a meshwork of proteins consisting primarily of collagen type IV, laminin, heparan sulfate proteoglycans, and nidogen^{24,25}. Surrounding this, but further from the endothelial cells, is a fibrillar matrix containing collagen type I²⁶. Neutrophil-ECM interactions occur directly through binding of neutrophil integrins to ECM proteins^{27,28} and indirectly via release of factors such as neutrophil proteases that remodel the ECM structure²⁹. These interactions support neutrophil chemotaxis^{30–32} and prevent apoptosis^{33,34}. Thus, the ECM is not simply a passive 3D scaffold but an active source of signals which sustains the inflammatory response³⁵. Physiological ECM composition in organ-on-a-chip models is therefore important to understand how neutrophils navigate these matrices to reach the inflammatory site.

Although some organ-on-a-chip models have incorporated an endothelial component, this is usually a 2D sheet of endothelial cells on a porous membrane^{12,21} rather than a 3D vessel against a 3D ECM. A few groups have produced 3D neutrophil transmigration models^{36–39}, investigating the role of chemoattractants, ECM pH, and endothelial cell type, but to our knowledge none have yet investigated the effect of ECM composition on endothelial and neutrophil responses to inflammation or inhibitors.

Here, we developed a novel model of neutrophil transmigration during inflammation, using the OrganoPlate system (Mimetas), a commercially available platform which has been used to model many organs already including the blood–brain barrier^{40,41}, liver^{42,43}, kidney^{44,45}, and gut^{46–48}, as well as the microvasculature^{49–51}. The OrganoPlate consists of either 40 or 96 chips in a 384-well plate format, allowing the screening of many conditions in a more robust, reproducible, and high-throughput way than in-house manufacturing of individual devices. The OrganoPlate has been used to investigate the infiltration of neutrophils through a collagen I gel⁵² towards an inflamed intestinal tube, however this model did not include an endothelial component. It has also been used to study monocyte adhesion to the endothelium⁵¹, but no transmigration was observed in this model. Neither model considered the effect of the ECM on cell phenotype.

In this study, we used this platform to explore the effects of different ECM composition on trans endothelial neutrophil migration. This work demonstrates the importance of considering choice of ECM when designing organ-on-a-chip models. The multi-well plate format of the OrganoPlate enabled testing of anti-inflammatory compounds, supporting a use for the model in screening potential drug candidates for diseases involving excessive neutrophil infiltration and inflammation.

Results

HUVEC form confluent vessels in OrganoPlates on geltrex with 25% collagen I. The neutrophil transmigration model was constructed in a Mimetas OrganoPlate 3-lane. The 3-lane OrganoPlate consists of a 384-well plate containing 40 chips, each with three channels. The channels are separated by Phaseguides, a liquid pinning technology which enables vessels to be grown against ECM, without any physical separation by membranes^{53,54} (Fig. 1a).

Two different ECMs, geltrex and collagen I, were compared in the OrganoPlate. Geltrex consists of a mix of proteins found physiologically in the endothelial basement membrane. However, when HUVEC were grown against geltrex alone, cells differentiated into tubes on the ECM, preventing proper vessel formation (Fig. 1b.i, Supplementary Movie 1). In contrast, when collagen I was used HUVEC grew on all four sides of the channel, forming confluent vessels (Fig. 1b.ii, Supplementary Movie 2), as previously reported^{49,55–58}. To produce a more physiologically relevant basement membrane without stimulating differentiation, a mixture of 75% geltrex and 25% collagen I was tested (referred to as geltrex mix from here). This prevented the tube formation seen with geltrex alone (Fig. 1b.iii, Supplementary Movie 3). Successful vessel formation was confirmed by staining of intercellular junctions and ability of vessels to retain 70 kDa dextrans (Fig. 1c).

TNF- α induces endothelial inflammation. To develop an inflammation model, vessels were grown in the top channel with ECM patterned into the middle channel. Stimulation of confluent vessels with TNF- α upregulated expression of ICAM-1 on the vessel surface (Fig. 2a). Analysis of cytokine release into supernatants from stimulated vessels showed upregulation of several inflammatory cytokines: soluble intercellular adhesion molecule-1 (ICAM-1), interleukin-8 (IL-8), C-X-C Motif Chemokine Ligand 1 (CXCL1), and C-C Motif Chemokine Ligand 2 (CCL2) (Fig. 2b). In contrast, macrophage migration inhibitory factor (MIF) and serine protease inhibitor E1 (SERPIN E1) were present in both unstimulated and stimulated samples. These data show that an inflammatory state was successfully induced in the vessels. There was no significant difference in cytokine expression between collagen I and geltrex mix, in either unstimulated or TNF- α stimulated vessels (Supplementary Fig. S2).

Neutrophils transmigrate upon inflammatory stimulation. Addition of freshly isolated human neutrophils into the inflamed vessels led to neutrophil transmigration out of the vessels and into the ECM (Fig. 3a.i). The use of human neutrophils increases the translational potential of this model, compared to use of immortalised cell lines. fMLP was added to the bottom channel to produce a gradient of chemoattractant for the neutrophils to migrate towards. Neutrophil transmigration was easily quantifiable by imaging due to the structure of the OrganoPlate, where the vessel and ECM are side by side. This allows straightforward analysis of both number of neutrophils transmigrated and the distance migrated within the ECM.

Very few neutrophils transmigrated across unstimulated vessels. Neutrophil transmigration differed between geltrex mix and collagen I ECMs. Fewer neutrophils transmigrated into collagen I, and post-transmigration neutrophils appeared unable to migrate towards the fMLP, stalling within 150 μm of the vessel. In contrast, neutrophils easily migrated throughout geltrex mix, covering the whole width of the gel channel during the 1.5-h experiment (Fig. 3a, Supplementary Fig. S3).

Interestingly, when the chemoattractant was not present, neutrophils still transmigrated into geltrex mix, although the number transmigrated was slightly reduced. In contrast, fMLP was required for transmigration into collagen I, with transmigration without fMLP comparable to unstimulated levels. The distance of migration in gel was not affected by presence of chemoattractant, in either geltrex mix or collagen I (Fig. 3b, Supplementary Fig. S3).

Pharmacological inhibition of neutrophil transmigration depends on vessel ECM. To investigate the potential of our model for testing anti-inflammatory or immunomodulatory compounds, we investigated the effect of inhibiting neutrophil proteases. A cocktail of protease inhibitors was used; an elastase inhibitor (sivelestat), a cathepsin G inhibitor (Cathepsin G Inhibitor 1), and a dual elastase and cathepsin G inhibitor (human recombinant SLPI). These were first tested in HUVEC-free OrganoPlates, to isolate their effect on neutrophil migration into the ECM. In this experiment, the ECM was plated 1 day before neutrophil addition. fMLP was added directly before neutrophil perfusion.

Neutrophils were unable to migrate into collagen I at all without HUVEC present (Fig. 4a). This suggests that the presence of HUVEC either makes the collagen I more permissible to migration, or that signalling between the HUVEC and neutrophils during transmigration activates the neutrophils and subsequently supports their migration. In contrast, neutrophils readily migrated into geltrex mix, when an fMLP gradient was present. This migration into geltrex mix was reduced by the protease inhibitor cocktail. The reduction seen was in numbers of neutrophils migrating rather than distance migrated in the ECM (Fig. 4b, Supplementary Fig. S4).

When HUVEC were incorporated into the model, number of neutrophils transmigrating into geltrex mix was inhibited by the protease inhibitor cocktail across (Fig. 4c). This inhibition was seen in all neutrophil donors tested. In contrast, this inhibition was not seen consistently in vessels grown against collagen I. Together, these data indicate that our inflammation-on-a-chip model can be used to explore the effect of potential immunomodulatory compounds. Moreover, these results indicate that the effects of such immunomodulatory compounds can vary depending on the underlying ECM.

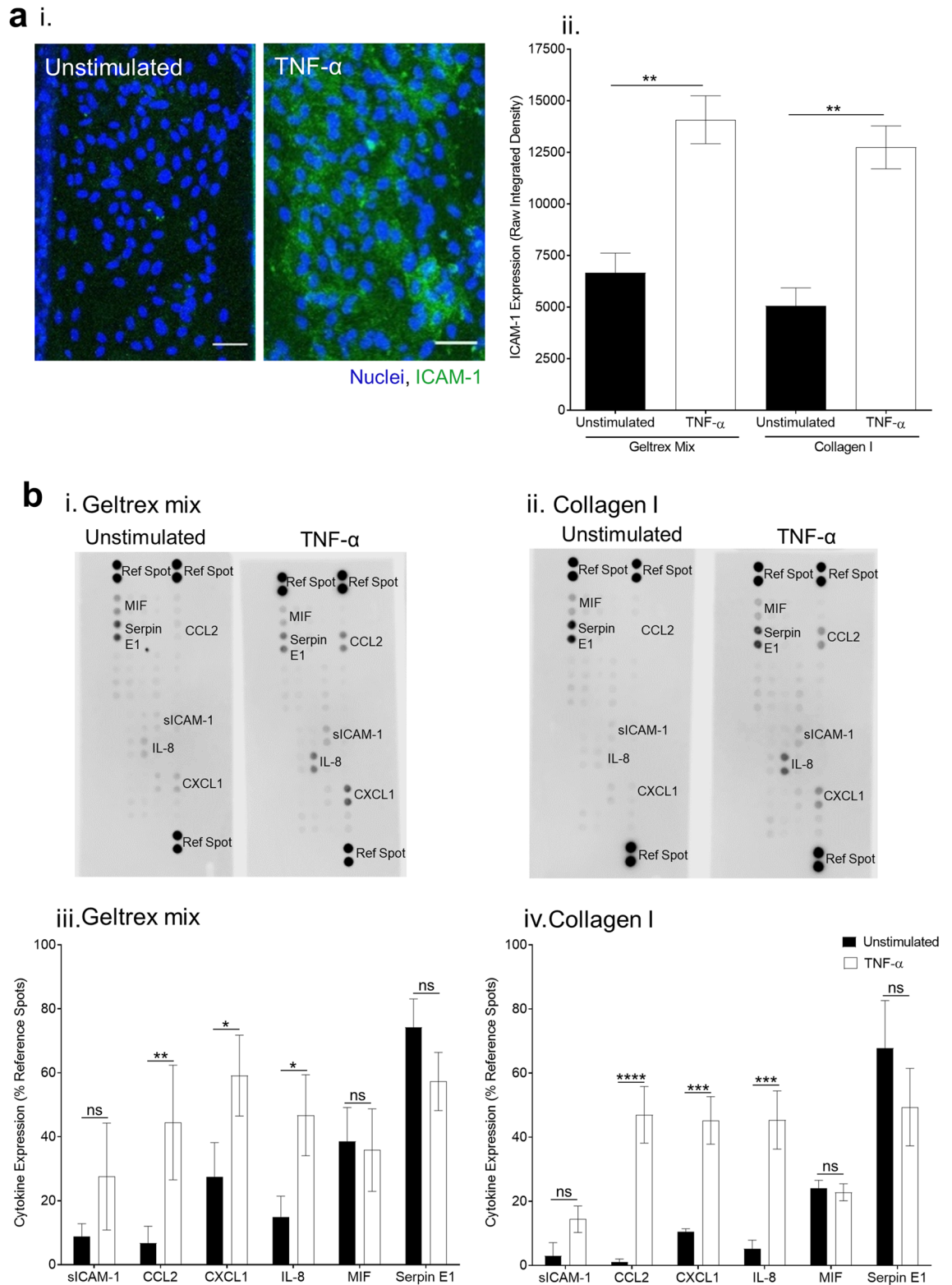
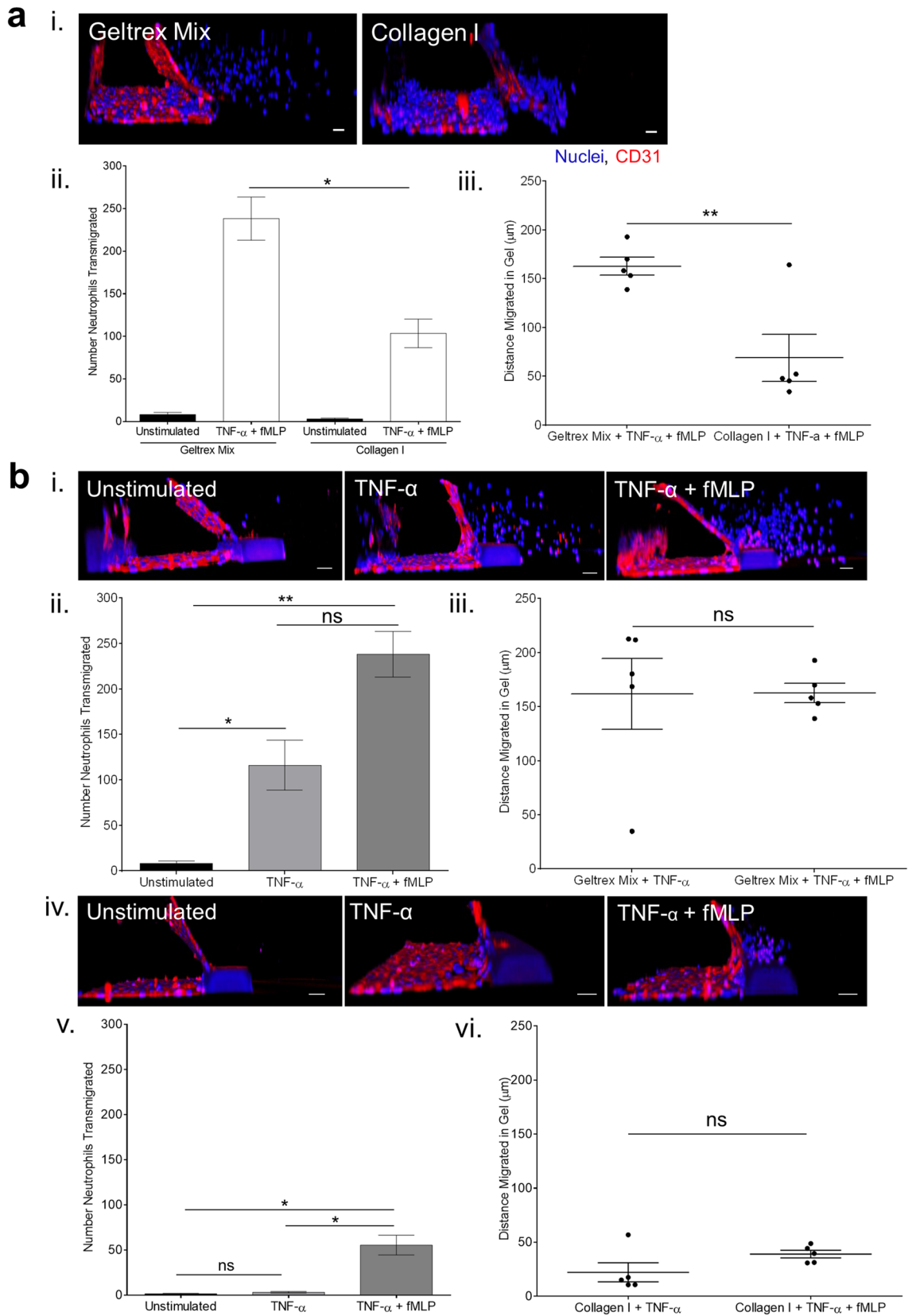


Figure 2. Tumour necrosis factor alpha (TNF- α) stimulation induces vessel expression of inflammatory molecules. (a) Stimulation of vessels with 1.6 ng/mL TNF- α induced Intercellular Adhesion Molecule 1 (ICAM-1) expression. i. Induction of ICAM-1 expression by TNF- α stimulation. Vessels were cultured for 1 week and then stimulated overnight with 1.6 ng/mL TNF- α . They were then fixed and stained with Hoechst-33342 (blue) and ICAM-1 (green). Images were obtained on a Leica SP5 confocal microscope. ii. Induction of ICAM-1 was quantified in FIJI. N = 5 independent experiments, mean \pm SEM, **P < 0.01. (b) Inflammatory cytokines were released by vessels upon TNF- α stimulation. Supernatants were taken from vessels 24 h post-TNF- α treatment. Cytokine expression was analysed from 5 pooled vessels per condition using a Human Cytokine Proteome Profiler Array with LI-COR infrared detection. i. Representative images of unstimulated vs TNF- α stimulated cytokine arrays. ii. Densitometry was performed in FIJI. N = 3 independent experiments, mean \pm SEM, ****P < 0.0001, ****P < 0.001, ***P < 0.01, *P < 0.05, ns = non-significant. Scale bars are representative of 50 μ m.



◀Figure 3. ECM composition affects characteristics of neutrophil transmigration across HUVEC vessels. **(a)** Transmigration of primary human neutrophils differs between geltrex mix and collagen I ECMs. Vessels were cultured for 1 week and then stimulated overnight with 1.6 ng/mL TNF- α . Neutrophils were isolated from human whole blood and added to the vessels for 1.5 h. *N*-formyl-methionyl-leucyl-phenylalanine (fMLP) was added to the bottom channel to generate a chemotactic gradient. Vessels were then fixed and stained with Hoechst-33342 (blue) and α -CD31 (red). Z-stacks were taken on a Leica SP5 confocal microscope. 3D reconstructions were generated in FIJI. Number/distance of neutrophils transmigrated was analysed using the Cell Counter plug in in FIJI. i. TNF- α stimulated HUVEC vessels supported neutrophil transmigration up an fMLP gradient. ii. More neutrophils transmigrated into geltrex mix than collagen I. iii. Neutrophils migrated further in geltrex mix than collagen I. **(b)** An fMLP chemotactic gradient was necessary for transmigration into collagen I but not geltrex mix. Neutrophil transmigration experiments were performed as described in part a, with or without the fMLP gradient present. i. Representative 3D reconstructions of neutrophil transmigration into geltrex mix. ii. In geltrex mix, presence of an fMLP gradient increased the number of neutrophils transmigrating. iii. Distance migrated in geltrex was not affected by fMLP. iv. Representative 3D reconstructions of neutrophil transmigration into collagen I. v. In collagen I, fMLP was required for neutrophils to transmigrate. vi. Distance migrated in collagen I was not affected by fMLP. N = 5 independent experiments/blood donors with n = 1–3 chips per condition, mean \pm SEM, ns = non-significant, *P < 0.05, **P < 0.01. Scale bars are representative of 50 μ m.

Discussion

In this study we present a new 3D in vitro model of neutrophil transendothelial migration and ECM infiltration. Confluent endothelial vessels were successfully cultured against two different types of ECM. The endothelial cells were stimulated to mimic an inflammatory state, leading to primary human neutrophil transmigration into the ECM. Significant differences were found between neutrophil transmigration into the different ECMs, including differences in response to pharmacological inhibition. This work highlights the ECM as an important modulator of cell phenotype, and ECM composition should therefore be considered carefully when designing complex in vitro models.

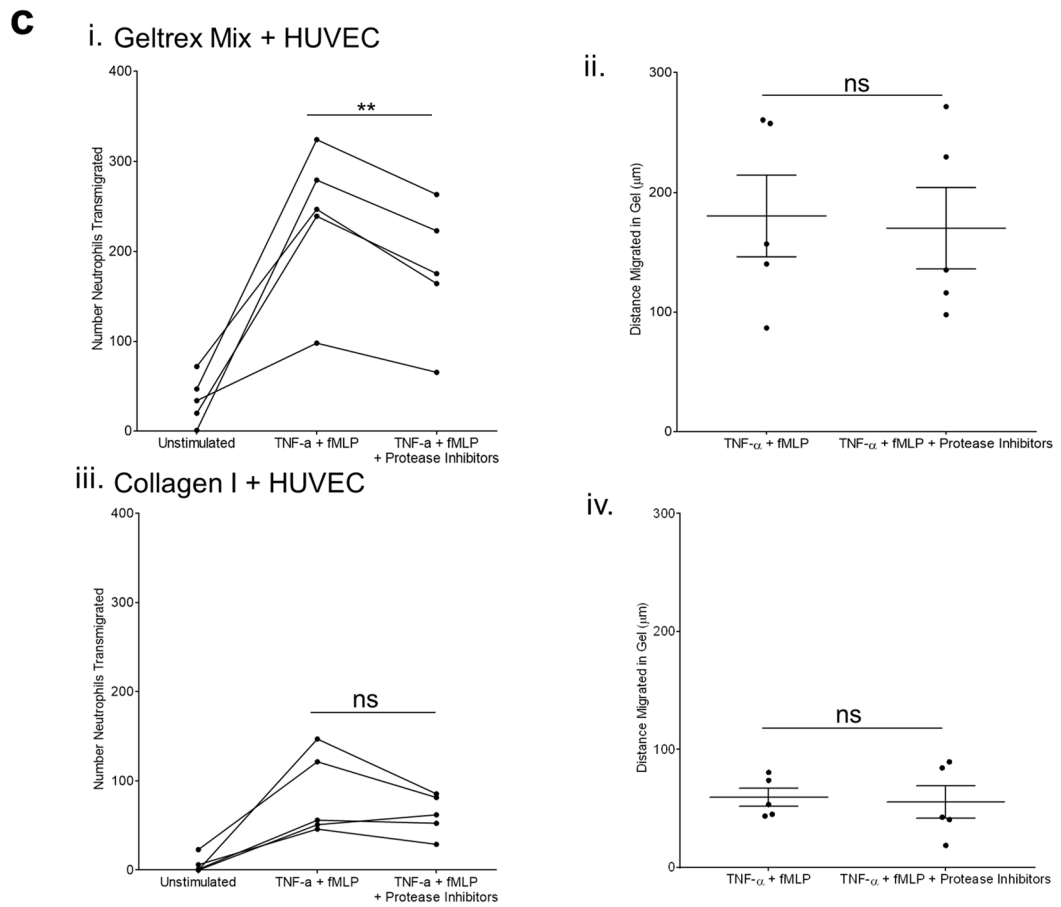
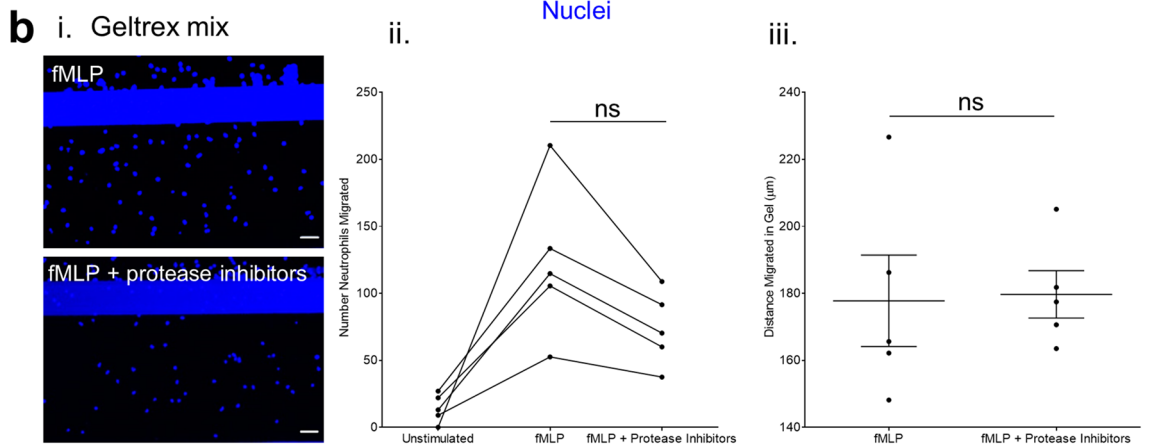
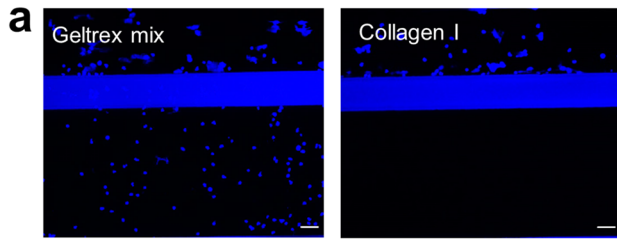
The Mimetas 3-lane OrganoPlate was chosen as the platform for the model, as it allows culture of cells under perfusion and against a 3D ECM without any physical separation by membranes or barriers^{53,54}. This is important when studying direct cell-ECM interactions and cell migration across the vessel wall. The three-lane structure allows the endothelium to be accessed both apically and basally. Therefore, inflammatory stimuli can be added in a physiologically relevant manner. For example, in our model we established an fMLP gradient across the ECM to mimic signals from the site of inflammation. A caveat to the use of this system is that the flow present is bidirectional rather than the physiological unidirectional. Previous studies have found that endothelial cells do not elongate or align in the direction of flow when it is bidirectional^{59,60}, and express higher levels of inflammatory cytokines than when under unidirectional flow⁶⁰. However, the presence of bidirectional flow is favorable over static as it allows the rolling of neutrophils over the endothelium, a key step in the process of transmigration in vivo⁶¹. In addition, the convenience of a pump free system and the 384-well plate format allows higher throughput experiments and enables testing of many conditions simultaneously, making this system attractive for drug screening.

ECM composition is a major regulator of neutrophil infiltration and yet physiologically relevant ECM are often overlooked in favour of experimentally convenient substrates. Two types of ECM were tested in the model, collagen I and geltrex. Collagen I is well established as a 2D coating or 3D ECM for endothelial cells, as it robustly supports adherence and monolayer formation^{49,55–58}. In contrast, studies on culturing endothelial cells on basement membrane extracts (BMEs) such as geltrex or matrigel focus on induction of tube formation, modelling angiogenesis^{62–64}. Our initial findings mirror these approaches, with successful vessel formation on collagen I, and vessel retraction and tube formation against geltrex. However, by combining geltrex with a small amount of collagen I we were able to create an ECM composition that supported vessel formation. Physiologically, the ECM consists of a thinner layer of basement membrane similar to geltrex, with a thicker layer of interstitial collagen I matrix below. Although our in vitro model does not recapitulate this bilayer, we are able to successfully culture vessels on a mixed matrix, exposing endothelial cells to a wider range of ECM components.

The difference in endothelial phenotype between collagen I and BMEs is probably due to multiple factors, including differences in stiffness of the gels and protein composition. A previous study cultured HUVEC on polyacrylamide gels, and found that as stiffness of the gel decreased HUVEC tended to undergo tube formation, but maintained monolayer formation at a higher stiffness⁶⁵. Other studies have found the basement membrane protein laminin to play an important role in determining monolayer vs tube formation^{66–68}. The basement membrane therefore influences endothelial phenotype, and so 3D models on ECM components have an opportunity to better represent the physiological microenvironment than 2D cultures, or 3D models on a single type of matrix protein.

Inflammation was induced in the vessels using TNF- α , a commonly used inflammatory stimulus, although other inflammatory stimuli could be readily compared in future studies. Immunofluorescence staining of surface ICAM-1, a key receptor for neutrophil binding, showed a significant upregulation upon stimulation. Analysis of vessel supernatants found induction of four inflammatory cytokines—soluble ICAM-1, CXCL1, CCL2 and IL-8. These cytokines have established roles in neutrophil transmigration^{69–72} and inflammatory diseases^{73–76} in vivo. Therefore, TNF- α was an appropriate stimulus for our model.

When neutrophils were added to stimulated vessels, differences in transmigration were observed depending on the ECM used. The first major difference seen was that many more neutrophils transmigrated into geltrex



◀Figure 4. Inhibition of neutrophil proteases. **(a)** Neutrophils are unable to migrate into collagen I without presence of HUVEC vessel. Maximum projections of ECM Z stacks. ECMs were patterned into the middle channel and incubated overnight with media in the top channel. Neutrophils were isolated from whole blood and added to the vessels for 1.5 h. fMLP was added to the bottom channel to generate a chemotactic gradient. ECMs were fixed and nuclei stained with Hoechst-33342 (blue). Z-stacks were taken on a Leica SP5 confocal microscope. **(b)** Number of neutrophils migrating into geltrex mix is reduced by protease inhibitors but distance migrated in ECM is unaffected. ECMs were patterned into the middle channel and incubated overnight with media in the top channel. Neutrophils were isolated from whole blood and incubated with protease inhibitors for 15 min before being added to the vessels for 1.5 h. fMLP was added to the bottom channel to generate a chemotactic gradient. ECMs were fixed and nuclei stained with Hoechst-33342 (blue). Z-stacks were taken on a Leica SP5 confocal microscope. Number (ii)/distance (iii) of neutrophils migrated was analysed using the Cell Counter plug in in FIJI. **(c)** Effect of protease inhibitors on neutrophil transmigration. Vessels were cultured for 1 week and then stimulated overnight with 1.6 ng/mL TNF- α . Neutrophils were isolated from whole blood and incubated with protease inhibitors for 15 min before being added to the vessels for 1.5 h. fMLP was added to the bottom channel to generate a chemotactic gradient. Vessels were then fixed and stained with Hoechst-33342 and α -CD31. Z-stacks were taken on a Leica SP5 confocal microscope. Number (ii,iii)/distance (iii,iv) of neutrophils migrated was analysed using the Cell Counter plug in in FIJI. N = 5 independent experiments/blood donors, n = 1–4 chips per condition, mean \pm SEM, ns = non-significant, **P < 0.01. Scale bars are representative of 50 μ m.

mix than collagen I, suggesting that vessels are more permissive to transmigration on geltrex mix. There is very little data directly comparing transmigration across endothelium on substrates of different protein composition, likely due to the propensity of HUVEC to undergo tube formation when cultured on BMEs. Studies have found that increasing stiffness of the ECM increases neutrophil transmigration^{77,78}, and that this corresponds to changes in stability of cell–cell junctions, alongside increased upregulation of inflammatory markers and vascular permeability^{79–81}. However, we found no difference in surface ICAM-1 or cytokine induction between the ECMs. It is possible that the differences we observe between the ECMs are due to the different protein compositions of geltrex mix and collagen I. Geltrex mix contains many different ECM components and growth factors that could alter HUVEC phenotype independently of mechanotransduction, demonstrating the importance of ECM composition in modelling inflammation.

Following transmigration, ability of neutrophils to infiltrate the ECM was hindered in collagen I compared to geltrex mix. This could again be due to mechanical differences between the ECMs, such as stiffness or pore size. Several groups have compared the structure of polymerized collagen I to BME gels, finding that although BME gels have smaller pores they are more deformable than collagen I matrices^{82,83}. Furthermore, it could be that geltrex mix contains more binding sites for the neutrophils and therefore supports their migration. Previous studies have found that binding of neutrophils to ECM proteins such as laminin and mindin promotes their chemotaxis towards the inflammatory site^{84,85}.

We also explored the requirement for a chemoattractant gradient in the model. Absence of fMLP in chips with geltrex mix did not significantly affect numbers or distance of neutrophils transmigrated. In contrast, vessels grown against collagen I required the presence of fMLP for induction of neutrophil transmigration. Geltrex mix itself does not induce neutrophil infiltration, as no neutrophil migration was observed into geltrex mix without HUVEC or fMLP present. Therefore, the threshold for induction of transmigration differs between the ECMs, with transmigration into collagen I requiring an extra inflammatory signal to direct the neutrophils across the endothelium.

We next investigated a role for neutrophil proteases in navigating the ECM post-transmigration. Whereas some reports suggest that neutrophils move passively through the basement membrane, favouring ‘low expression regions’ with lower protein concentration^{86–88}, other studies support a role for neutrophils in releasing proteases to actively degrade the BM^{31,89–91}. We first observed that neutrophils were unable to penetrate a collagen I matrix without HUVEC present, which suggests a role for the endothelium in supporting migration into the ECM. This could be due to activation or priming of the neutrophils during transmigration. Previous studies have found that post-transmigration neutrophils have an altered phenotype, including increased motility⁹², increased CD11b/CD18 expression^{92,93}, and an increased ability to migrate through pericyte layers⁹⁴. Alternatively, it could be that the HUVEC alter the underlying ECM, either by remodelling or by depositing their own ECM during culture. The ability of endothelial cells to degrade the ECM during angiogenesis is well established^{95–97}, but whether remodelling of the ECM occurs in mature vessels is more uncertain.

In contrast to collagen I, neutrophils easily migrated into geltrex mix without presence of a vessel. Moreover, inhibiting elastase and cathepsin G moderately reduced this infiltration, demonstrating a contribution from neutrophil proteases. When the inhibitors were tested with vessels present, a modest but consistent inhibition of migration was seen in geltrex mix vessels. This was not seen in vessels formed on collagen I. This suggests that elastase and cathepsin G are partially responsible for enabling migration in geltrex mix. Other proteases such as matrix metalloproteinases (MMPs) have also been found to play a role in neutrophil infiltration, and may also play a role here^{98–100}. The lack of effect in collagen I could indicate that these proteases are not involved in collagen I degradation, although there is evidence that in cell-free systems that both enzymes are able to perform this function^{101,102}.

Our results emphasise the role of the ECM in modulating cell phenotype and response to inhibitors. Previous studies, particularly in the field of cancer, have also found that 3D environment and ECM composition affect drug efficacy. For example, several groups have found cancer cells to be less responsive to chemotherapy in 3D cultures than in 2D monolayers^{103,104}, with one finding that fibronectin as a substrate increased the lack of responsiveness compared to collagen I¹⁰³, and another showing increased resistance to chemotherapy in

biological matrices compared to synthetic matrices¹⁰⁴. These studies highlight that the ECM is a source of both mechanical and biological signals. Therefore, typical 2D cell cultures cannot accurately be used to test responses to drugs. Complex 3D models which recapitulate the *in vivo* microenvironment are needed for drug discovery. For example, inflammatory sites are often characterised by increased matrix stiffness¹⁰⁵, which has been found to increase inflammation¹⁰⁶ and reduce drug efficacy¹⁰⁷. Future models could tailor ECM composition to each organ, disease, or person. Creation of bespoke ECM compositions will enable development of accurate models to increase understanding of cell behaviour in disease, and support drug development.

Conclusions

3D *in vitro* organ on a chip models have the potential to bridge the gap between current *in vitro* and *in vivo* models. Development of these models requires knowledge of the microenvironment being modelled, including the physical 3D structure and the cell types and signals present. Inflammatory diseases are often characterised by excessive neutrophil infiltration and associated ECM remodelling. Here, we have successfully established a neutrophil transmigration on a chip model where neutrophils transmigrate out of an endothelial vessel and through a 3D ECM environment, as they would *in vivo*. We found substantial differences in characteristics of neutrophil transmigration depending on the ECM used, including different responses to inhibitors. This work highlights how extracellular components influence cell behaviour, and demonstrates a need for accurate recapitulation of *in vivo* microenvironments when designing *in vitro* models. Further work is required to fine-tune ECM structures for use in models and to delineate exactly how the ECM alters cell phenotype.

Materials and methods

All materials were obtained from Sigma (UK) unless specified otherwise.

All experiments involving human participants was reviewed by the Human Biology Research Ethics Committee, University of Cambridge, with fully-informed, written consent in accordance with the Declaration of Helsinki.

HUVEC culture. Human umbilical vein endothelial cells (HUVEC, PromoCell, Germany) were cultured in Endothelial Growth Medium (Media, PromoCell) with 30 µg/mL gentamicin, in T25 or T75 tissue culture flasks. Cells were grown to confluence (37 °C, 5% CO₂) and then passaged using PromoCell Detach Kit. HUVEC were used at passage 4.

Extracellular matrix (ECM) compositions. For collagen I ECM, 5 mg/mL rat tail collagen type I (ibidi, Germany) was neutralised by mixing at a ratio of 8:1:1 with 1 M HEPES and 37 g/L NaHCO₃ producing a 4 mg/mL solution. For geltrex mix ECM, Geltrex™ LDEV-Free Reduced Growth Factor Basement Membrane Matrix (Gibco, A1413302) was diluted to 14.6 mg/mL in media and then mixed at a ratio of 75:25 (v/v) with 3 mg/mL collagen I. 3 mg/mL collagen I was made by neutralisation of 5 mg/mL collagen I with 1 M NaOH and 7.5% (w/v) NaHCO₃ as per the manufacturer's protocol. For each batch of geltrex, preliminary screening experiments were performed to confirm successful vessel formation. Some batches of geltrex required additional coating of the ECM with 10 µg/mL fibronectin for 2 days to support HUVEC adhesion.

OrganoPlate® culture. Three-lane OrganoPlates® (Mimetas, 4003-400B, Netherlands) were used. 50 µL Hanks' Balanced Salt Solution (without calcium and magnesium, HBSS, Gibco) was added to the observation windows to prevent chips from drying out. 1.75 µL geltrex mix or 1.85 µL collagen I was added to the middle lane of the chip via the gel inlet (Fig. 1a). ECMs were polymerised for 10 min (37 °C, 5% CO₂), then 50 µL HBSS was added to the gel inlet to prevent ECM dehydration. Chips were incubated for a further 50 min, after which HBSS was aspirated from the gel inlets.

HUVEC were seeded into the top channel by addition of 2 µL cell suspension at 2 × 10⁷/mL. Media was added to the top channel inlet and the plate incubated for 2 h on its side at a 70° angle (37 °C, 5% CO₂) to allow cells to attach to the ECM. Media was then added to the top channel outlet and perfusion begun (8 min intervals, 7° angle) on the Mimetas OrganoFlow S plate rocker. Plates were incubated under perfusion for 7 days to enable optimal barrier function of the vessels. Media was refreshed every 2–3 days.

Barrier Integrity Assay. After 7 days of incubation, the barrier function of the vessels was tested. 0.5 mg/mL 70 kDa tetramethylrhodamine (TRITC)-dextran was added to the top channel for 30 min. Dye retention was imaged on a Leica SP5 confocal microscope. Barrier function was quantified by measuring the fluorescence in each channel in FIJI¹⁰⁸ and then calculating the ratio of fluorescence in the vessel channel versus fluorescence in the ECM channel.

Neutrophil isolation. Blood was taken from volunteers by venepuncture into 3.8% (v/v) sodium citrate-containing vacutainers (Greiner Bio-One). The volunteers were healthy and free of medication for at least 10 days prior to venepuncture. Fully-informed, written consent was obtained in accordance with the Declaration of Helsinki, and use of blood was reviewed by the Human Biology Research Ethics Committee, University of Cambridge. Nine mL blood was layered onto 5 mL histopaque-1077 and then centrifuged (428g, 30 min, room temperature, no brake). All layers above the red blood cell pellet were aspirated and the pellet diluted 1:1 (v/v) with HBSS, and then further diluted 1:1 (v/v) with 2% (w/v) dextran. The resulting solution was left at room temperature for 45 min to allow red blood cells to sediment. The opaque top layer was removed and diluted 1:1 (v/v) with HBSS and then centrifuged (200g, 10 min, room temperature, medium braking/acceleration). The

pellet was resuspended in 1 mL sterile, deionized water for 45 s to lyse residual red blood cells, then topped up to 15 mL with HBSS and centrifuged again (200g, 10 min, room temperature, medium braking/acceleration). The resulting neutrophil pellet was resuspended at 3.75×10^6 /mL in Roswell Park Memorial Institute (RPMI) 1640 medium containing 10% (v/v) foetal calf serum.

Neutrophil transmigration in OrganoPlates®. On day 7 of culture, vessel lumens were stimulated with 1.6 ng/mL human recombinant tumour necrosis factor- α (TNF- α) (R&D Systems) overnight. Immediately before neutrophil perfusion, the bottom channels of the chips were filled with 200 nM *N*-formyl-methionyl-leucyl-phenylalanine (fMLP). Neutrophils were then added to the vessels for 1.5 h on the rocker (37 °C, 5% CO₂). The number of independent neutrophil donors used are specified in the figure legends.

Protease inhibitor treatments. A cocktail of 100 μ M sivelestat (Biotechne), 10 μ M Cathepsin G Inhibitor 1 (Cambridge Bioscience), and 250 nM human recombinant secretory leukocyte peptidase inhibitor (SLPI) (Biotechne) was used. Neutrophils were incubated with the inhibitors or 0.2% (v/v) DMSO vehicle control for 15 min at room temperature before addition to the OrganoPlate®.

Immunofluorescence. Vessels were fixed with 4% (w/v) paraformaldehyde (Santa Cruz Biotechnology) for 15 min, washed twice for five minutes with PBS and then blocked with 2% (w/v) BSA for 30 min. Anti-CD31 antibody (Abcam, ab9498) in 2% (w/v) BSA was added and incubated overnight at room temperature on a plate rocker. Vessels were washed twice with PBS and then anti-mouse-647 (ThermoFisher) secondary antibody, Hoechst-33342 (ThermoFisher), and phalloidin-FITC (ThermoFisher) were added and incubated for 1.5 h at room temperature in the dark, on a rocker. Two more PBS washes were performed. Images were obtained on a Leica SP5 confocal microscope, using a 20 \times objective. 3D reconstructions were created in FIJI¹⁰⁹. Neutrophil transmigration was quantified in FIJI using the Cell Counter plug in. A neutrophil was considered transmigrated if it was to the right of the endothelial barrier, which was identified by CD31 staining (Supplementary Fig. S1). Neutrophils co-localised with CD31 staining were not considered transmigrated.

Cytokine arrays. R&D Systems Cytokine Proteome Profiler Arrays were used to investigate cytokine production. Supernatants were taken from five chips 24 h after TNF- α stimulation and pooled together. Cytokine arrays were carried out as per manufacturer's instructions, with the modified protocol for detection using AlexaFluor™ 790 Streptavidin (ThermoFisher). A LI-COR Odyssey Fc was used for detection of arrays. Cytokine levels were quantified by densitometry in FIJI. Cytokine expression was expressed as a % of the positive reference spots for each array.

Statistical analysis. Statistical analysis was performed in GraphPad Prism v9. All tests were carried out using matched analyses. Two-way ANOVA with Sidak's multiple comparisons test was used to analyse differences in surface ICAM-1 levels, cytokine expression, or number of neutrophils transmigrated between collagen I and geltrex mix, and unstimulated versus TNF- α stimulated. One-way ANOVA with Tukey's multiple comparisons test was used to compare differences in number of neutrophils transmigrated between unstimulated, TNF- α , and TNF- α + fMLP, and also to compare unstimulated, stimulated, and protease inhibitor-treated conditions. For differences in distance of neutrophil migration, paired two-tailed t tests were used. Values $P < 0.05$ were considered significant. In figure legends, N refers to independent experiments/neutrophil donors, and n refers to technical repeats (number of vessels) within donors.

Data availability

Data are available from the corresponding author on reasonable request.

Received: 24 December 2021; Accepted: 11 March 2022

Published online: 27 April 2022

References

1. Filippi, M. D. Neutrophil transendothelial migration: Updates and new perspectives. *Blood* **133**, 2149–2158 (2019).
2. Margraf, A., Ley, K. & Zarbock, A. Neutrophil recruitment: From model systems to tissue-specific patterns. *Trends Immunol.* **40**, 613–634 (2019).
3. Yamahashi, Y. *et al.* Integrin associated proteins differentially regulate neutrophil polarity and directed migration in 2D and 3D. *Biomed. Microdevices.* **17**, 100 (2015).
4. Boyden, S. The chemotactic effect of mixtures of antibody and antigen on polymorphonuclear leucocytes. *J. Exp. Med.* **115**, 453–466 (1962).
5. Mestas, J. & Hughes, C. C. W. Of mice and not men: Differences between mouse and human immunology. *J. Immunol.* **172**, 2731–2738 (2004).
6. Doeing, D. C., Borowicz, J. L. & Crockett, E. T. Gender dimorphism in differential peripheral blood leukocyte counts in mice using cardiac, tail, foot, and saphenous vein puncture methods. *BMC Clin. Pathol.* **3**, 3 (2003).
7. Modi, W. S. & Yoshimura, T. Isolation of novel GRO genes and a phylogenetic analysis of the CXC chemokine subfamily in mammals. *Mol. Biol. Evol.* **16**, 180–193 (1999).
8. Seyhan, A. A. Lost in translation: the valley of death across preclinical and clinical divide—Identification of problems and overcoming obstacles. *Transl. Med. Commun.* **4**, 1–19 (2019).
9. Low, L. A., Mummery, C., Berridge, B. R., Austin, C. P. & Tagle, D. A. Organs-on-chips: Into the next decade. *Nat. Rev. Drug Discov.* <https://doi.org/10.1038/s41573-020-0079-3> (2020).
10. Wu, Q. *et al.* Organ-on-a-chip: Recent breakthroughs and future prospects. *Biomed. Eng. Online* **19**, 1–19 (2020).

11. Liu, C., Oikonomopoulos, A., Sayed, N. & Wu, J. C. Modeling human diseases with induced pluripotent stem cells: From 2D to 3D and beyond. *Dev.* **145**, dev156166 (2018).
12. Huh, D. *et al.* Reconstituting organ-level lung functions on a chip. *Science* (80-). **328**, 1662–1668 (2010).
13. Benam, K. H. *et al.* Small airway-on-a-chip enables analysis of human lung inflammation and drug responses in vitro. *Nat. Methods* **13**, 151–157 (2016).
14. Benam, K. H. *et al.* Matched-comparative modeling of normal and diseased human airway responses using a microengineered breathing lung chip. *Cell Syst.* **3**, 456–466.e4 (2016).
15. Marsano, A. *et al.* Beating heart on a chip: A novel microfluidic platform to generate functional 3D cardiac microtissues. *Lab Chip* **16**, 599–610 (2016).
16. Liu, H. *et al.* Heart-on-a-chip model with integrated extra- and intracellular bioelectronics for monitoring cardiac electrophysiology under acute hypoxia. *Nano Lett.* **20**, 2585–2593 (2020).
17. Abulaiti, M. *et al.* Establishment of a heart-on-a-chip microdevice based on human iPS cells for the evaluation of human heart tissue function. *Sci. Rep.* **10**, 19201 (2020).
18. Ho, C. T. *et al.* Liver-cell patterning Lab Chip: Mimicking the morphology of liver lobule tissue. *Lab Chip* **13**, 3578–3587 (2013).
19. Du, Y. *et al.* Mimicking liver sinusoidal structures and functions using a 3D-configured microfluidic chip. *Lab Chip* **17**, 782–794 (2017).
20. Schutgens, F. *et al.* Tubuloids derived from human adult kidney and urine for personalized disease modeling. *Nat. Biotechnol.* **37**, 303–313 (2019).
21. Kwak, B. S. *et al.* Microfluidic skin chip with vasculature for recapitulating the immune response of the skin tissue. *Biotechnol. Bioeng.* **117**, 1853–1863 (2020).
22. Wufuer, M. *et al.* Skin-on-a-chip model simulating inflammation, edema and drug-based treatment. *Sci. Rep.* **6**, 1–12 (2016).
23. Ramadan, Q. & Ting, F. C. W. In vitro micro-physiological immune-competent model of the human skin. *Lab Chip* **16**, 1899–1908 (2016).
24. Jayadev, R. & Sherwood, D. R. Basement membranes. *Curr. Biol.* **27**, R207–R211 (2017).
25. Leclech, C., Natale, C. F. & Barakat, A. I. The basement membrane as a structured surface—Role in vascular health and disease. *J. Cell Sci.* **133**, jcs239889 (2021).
26. Witjas, F. M. R., van den Berg, B. M., van den Berg, C. W., Engelse, M. A. & Rabelink, T. J. Concise review: The endothelial cell extracellular matrix regulates tissue homeostasis and repair. *Stem Cells Transl. Med.* **8**, 375–382 (2019).
27. Sheikh, S. *et al.* Differing mechanisms of leukocyte recruitment and sensitivity to conditioning by shear stress for endothelial cells treated with tumour necrosis factor-alpha or interleukin-1beta. *Br. J. Pharmacol.* **145**, 1052–1061 (2005).
28. Werr, J., Xie, X., Hedqvist, P., Ruoslahti, E. & Lindbom, L. $\beta 1$ integrins are critically involved in neutrophil locomotion in extravascular tissue in vivo. *J. Exp. Med.* **187**, 2091–2096 (1998).
29. Mezu-Ndubuisi, O. J. & Maheshwari, A. The role of integrins in inflammation and angiogenesis. *Pediatr. Res.* **89**, 1619–1626 (2021).
30. Steadman, R. *et al.* Laminin cleavage by activated human neutrophils yields proteolytic fragments with selective migratory properties. *J. Leukoc. Biol.* **53**, 354–365 (1993).
31. Mydel, P. *et al.* Neutrophil elastase cleaves laminin-332 (laminin-5) generating peptides that are chemotactic for neutrophils. *J. Biol. Chem.* **283**, 9513–9522 (2008).
32. Lin, M. *et al.* Matrix metalloproteinase-8 facilitates neutrophil migration through the corneal stromal matrix by collagen degradation and production of the chemotactic peptide pro-gly-pro. *Am. J. Pathol.* **173**, 144–153 (2008).
33. Kettritz, R. *et al.* Extracellular matrix regulates apoptosis in human neutrophils. *Kidney Int.* **55**, 562–571 (1999).
34. Ginis, I. & Faller, D. V. Protection from apoptosis in human neutrophils is determined by the surface of adhesion. *Am. J. Physiol.* **272**, C295–309 (1997).
35. Korpos, E., Wu, C., Song, J., Hallmann, R. & Sorokin, L. Role of the extracellular matrix in lymphocyte migration. *Cell Tissue Res.* **339**, 47–57 (2010).
36. Ingram, P. N., Hind, L. E., Jiminez-Torres, J. A., Huttenlocher, A. & Beebe, D. J. An accessible organotypic microvessel model using iPSC-derived endothelium. *Adv. Healthc. Mater.* **7**, 10.1002/adhm.201700497 (2018).
37. McMinn, P. H., Hind, L. E., Huttenlocher, A. & Beebe, D. J. Neutrophil trafficking on-a-chip: An in vitro, organotypic model for investigating neutrophil priming, extravasation, and migration with spatiotemporal control. *Lab Chip* **19**, 3697–3705 (2019).
38. Han, S. *et al.* A versatile assay for monitoring in vivo-like transendothelial migration of neutrophils. *Lab Chip* **12**, 3861–3865 (2012).
39. Chen, M. B. *et al.* On-chip human microvasculature assay for visualization and quantification of tumor cell extravasation dynamics. *Nat. Protoc.* **12**, 865–880 (2017).
40. Wevers, N. R. *et al.* A perfused human blood-brain barrier on-a-chip for high-throughput assessment of barrier function and antibody transport. *Fluids Barriers CNS* **15**, 1–12 (2018).
41. Koo, Y., Hawkins, B. T. & Yun, Y. Three-dimensional (3D) tetra-culture brain on chip platform for organophosphate toxicity screening. *Sci. Rep.* **8**, 1–7 (2018).
42. Bircsak, K. M. *et al.* A 3D microfluidic liver model for high throughput compound toxicity screening in the OrganoPlate*. *Toxicology* **450**, 152667 (2021).
43. Jang, M., Kleber, A., Ruckelshausen, T., Betzholz, R. & Manz, A. Differentiation of the human liver progenitor cell line (HepaRG) on a microfluidic-based biochip. *J. Tissue Eng. Regen. Med.* **13**, 482–494 (2019).
44. Petrosyan, A. *et al.* A glomerulus-on-a-chip to recapitulate the human glomerular filtration barrier. *Nat. Commun.* **10**, 1–17 (2019).
45. Vormann, M. K. *et al.* Nephrotoxicity and kidney transport assessment on 3D perfused proximal tubules. *AAPS J.* **20**, 1–11 (2018).
46. Naumovska, E. *et al.* Direct on-chip differentiation of intestinal tubules from induced pluripotent stem cells. *Int. J. Mol. Sci.* **21**, 1–15 (2020).
47. Gijzen, L. *et al.* An intestine-on-a-chip model of plug-and-play modularity to study inflammatory processes. *SLAS Technol.* **25**, 585–597 (2020).
48. Beurivage, C. *et al.* Development of a human primary gut-on-a-chip to model inflammatory processes. *Sci. Rep.* **10**, 1–16 (2020).
49. Van Duinen, V. *et al.* 96 perfusable blood vessels to study vascular permeability in vitro. *Sci. Rep.* **7**, 1–11 (2017).
50. van Duinen, V. *et al.* Perfused 3D angiogenic sprouting in a high-throughput in vitro platform. *Angiogenesis* **22**, 157–165 (2019).
51. Poussin, C. *et al.* 3D human microvessel-on-a-chip model for studying monocyte-to-endothelium adhesion under flow—Application in systems toxicology. *Altex* **37**, 47–63 (2020).
52. Gjorevski, N. *et al.* Neutrophilic infiltration in organ-on-a-chip model of tissue inflammation. *Lab Chip* **20**, 3365–3374 (2020).
53. Vulto, P. *et al.* Phaseguides: A paradigm shift in microfluidic priming and emptying. *Lab Chip* **11**, 1596–1602 (2011).
54. Trietsch, S. J., Israëls, G. D., Joore, J., Hankemeier, T. & Vulto, P. Microfluidic titer plate for stratified 3D cell culture. *Lab Chip* **13**, 3548–3554 (2013).
55. Yetkin-Arik, B. *et al.* Endothelial tip cells in vitro are less glycolytic and have a more flexible response to metabolic stress than non-tip cells. *Sci. Rep.* **9**, 1–17 (2019).

56. van Duinen, V. *et al.* Robust and scalable angiogenesis assay of perfused 3D human iPSC-derived endothelium for anti-angiogenic drug screening. *Int. J. Mol. Sci.* **21**, 4804 (2020).
57. Junaid, A. *et al.* Metabolic response of blood vessels to tnfa. *Elife* **9**, 1–28 (2020).
58. Ragelle, H. *et al.* Human retinal microvasculature-on-a-chip for drug discovery. *Adv. Healthc. Mater.* **9**, 2001531 (2020).
59. Lee, D. W., Choi, N. & Sung, J. H. A microfluidic chip with gravity-induced unidirectional flow for perfusion cell culture. *Biotechnol. Prog.* **35**, e2701 (2019).
60. Yang, Y. *et al.* Pumpless microfluidic devices for generating healthy and diseased endothelia. *Lab Chip* **19**, 3212–3219 (2019).
61. Maas, S. L., Soehnlein, O. & Viola, J. R. Organ-specific mechanisms of transendothelial neutrophil migration in the lung, liver, kidney, and aorta. *Front. Immunol.* **9**, 2739 (2018).
62. Russo, T. A., Banuth, A. M. M., Nader, H. B. & Dreyfuss, J. L. Altered shear stress on endothelial cells leads to remodeling of extracellular matrix and induction of angiogenesis. *PLoS ONE* **15**, e0241040 (2020).
63. Faulkner, A. *et al.* A thin layer angiogenesis assay: A modified basement matrix assay for assessment of endothelial cell differentiation. *BMC Cell Biol.* **15**, 41 (2014).
64. Lovecchio, J., Pannella, M., Giardino, L., Calzà, L. & Giordano, E. A dynamic culture platform enhances the efficiency of the 3D HUVEC-based tube formation assay. *Biotechnol. Bioeng.* **117**, 789–797 (2020).
65. Deroanne, C. F., Lapiere, C. M. & Nusgens, B. V. In vitro tubulogenesis of endothelial cells by relaxation of the coupling extracellular matrix-cytoskeleton. *Cardiovasc. Res.* **49**, 647–658 (2001).
66. Kubota, Y., Kleinman, H. K., Martin, G. R. & Lawley, T. J. Role of laminin and basement membrane in the morphological differentiation of human endothelial cells into capillary-like structures. *J. Cell Biol.* **107**, 1589–1598 (1988).
67. Stamati, K., Priestley, J. V., Mudera, V. & Cheema, U. Laminin promotes vascular network formation in 3D in vitro collagen scaffolds by regulating VEGF uptake. *Exp. Cell Res.* **327**, 68–77 (2014).
68. Shakado, S. *et al.* Effects of extracellular matrices on tube formation of cultured rat hepatic sinusoidal endothelial cells. *Hepatology* **22**, 969–973 (1995).
69. Kunisada, M., Hosaka, C., Takemori, C., Nakano, E. & Nishigori, C. CXCL1 inhibition regulates UVB-induced skin inflammation and tumorigenesis in Xpa-deficient mice. *J. Invest. Dermatol.* **137**, 1975–1983 (2017).
70. Reichel, C. A. *et al.* Ccl2 and Ccl3 mediate neutrophil recruitment via induction of protein synthesis and generation of lipid mediators. *Arterioscler. Thromb. Vasc. Biol.* **29**, 1787–1793 (2009).
71. Williams, A. E. *et al.* Evidence for chemokine synergy during neutrophil migration in ARDS. *Thorax* **72**, 66–73 (2017).
72. Tajima, A., Iwase, T., Shinji, H., Seki, K. & Mizunoe, Y. Inhibition of endothelial interleukin-8 production and neutrophil transmigration by *Staphylococcus aureus* beta-hemolysin. *Infect. Immun.* **77**, 327–334 (2009).
73. Hou, S. M. *et al.* CXCL1 contributes to IL-6 expression in osteoarthritis and rheumatoid arthritis synovial fibroblasts by CXCR2, c-Raf, MAPK, and AP-1 pathway. *Arthritis Res. Ther.* **22**, 1–11 (2020).
74. Dewald, O. *et al.* CCL2/monocyte chemoattractant protein-1 regulates inflammatory responses critical to healing myocardial infarcts. *Circ. Res.* **96**, 881–889 (2005).
75. Cotton, J. A. *et al.* Interleukin-8 in gastrointestinal inflammation and malignancy: Induction and clinical consequences. *Int. J. Interferon Cytokine Mediator Res.* **8**, 13–34 (2016).
76. Witkowska, A. M. Soluble ICAM-1: A marker of vascular inflammation and lifestyle. *Cytokine* **31**, 127–134 (2005).
77. Onken, M. D. *et al.* Endothelial monolayers and transendothelial migration depend on mechanical properties of the substrate. *Cytoskeleton* **71**, 695–706 (2014).
78. Stroka, K. M. & Aranda-Espinoza, H. Endothelial cell substrate stiffness influences neutrophil transmigration via myosin light chain kinase-dependent cell contraction. *Blood* **118**, 1632–1640 (2011).
79. Mambetsariev, I. *et al.* Stiffness-activated gef-h1 expression exacerbates lpsinduced lung inflammation. *PLoS ONE* **9**, e92670 (2014).
80. Meng, F. *et al.* Attenuation of lipopolysaccharide-induced lung vascular stiffening by lipoxin reduces lung inflammation. *Am. J. Respir. Cell Mol. Biol.* **52**, 152–161 (2015).
81. Huynh, J. *et al.* Age-related intimal stiffening enhances endothelial permeability and leukocyte transmigration. *Sci. Transl. Med.* **3**, 112–122 (2011).
82. Anguiano, M. *et al.* Characterization of three-dimensional cancer cell migration in mixed collagen-Matrigel scaffolds using microfluidics and image analysis. *PLoS ONE* **12**, e0171417 (2017).
83. Yadav, S. K. *et al.* Frontline science: Elevated nuclear lamin A is permissive for granulocyte transendothelial migration but not for motility through collagen I barriers. *J. Leukoc. Biol.* **104**, 239–251 (2018).
84. Jia, W., Li, H. & He, Y. W. The extracellular matrix protein mindin serves as an integrin ligand and is critical for inflammatory cell recruitment. *Blood* **106**, 3854–3859 (2005).
85. Adair-Kirk, T. L. *et al.* A site on laminin $\alpha 5$, AQARSAASKVKVSMKF, induces inflammatory cell production of matrix metalloproteinase-9 and chemotaxis. *J. Immunol.* **171**, 398–406 (2003).
86. Voisin, M. B., Pröbstl, D. & Nourshargh, S. Venular basement membranes ubiquitously express matrix protein low-expression regions: Characterization in multiple tissues and remodeling during inflammation. *Am. J. Pathol.* **176**, 482–495 (2010).
87. Poduval, P., Sillat, T., Virtanen, I., Dabagh, M. & Kontinen, Y. T. Immigration check for neutrophils in RA lining: Laminin $\alpha 5$ low expression regions act as exit points. *Scand. J. Rheumatol.* **39**, 132–140 (2010).
88. Wang, S. *et al.* Venular basement membranes contain specific matrix protein low expression regions that act as exit points for emigrating neutrophils. *J. Exp. Med.* **203**, 1519–1532 (2006).
89. Chua, F. Neutrophil elastase: Mediator of extracellular matrix destruction and accumulation. *Proc. Am. Thorac. Soc.* **3**, 424–427 (2006).
90. Kryczka, J. & Boncela, J. Proteases revisited: Roles and therapeutic implications in fibrosis. *Mediators Inflamm.* **2017**, 1–14 (2017).
91. Heck, L. W., Blackburn, W. D., Irwin, M. H. & Abrahamson, D. R. Degradation of basement membrane laminin by human neutrophil elastase and cathepsin G. *Am. J. Pathol.* **136**, 1267–1274 (1990).
92. Gonzalez, A. L., El-Bjeirami, W., West, J. L., McIntire, L. V. & Smith, C. W. Transendothelial migration enhances integrin-dependent human neutrophil chemokinesis. *J. Leukoc. Biol.* **81**, 686–695 (2007).
93. Paulsson, J. M., Jacobson, S. H. & Lundahl, J. Neutrophil activation during transmigration in vivo and in vitro A translational study using the skin chamber model. *J. Immunol. Methods* **361**, 82–88 (2010).
94. Ayres-Sander, C. E. *et al.* Transendothelial migration enables subsequent transmigration of neutrophils through underlying pericytes. *PLoS ONE* **8**, e60025 (2013).
95. Liu, J. *et al.* Synthetic extracellular matrices with tailored adhesiveness and degradability support lumen formation during angiogenic sprouting. *Nat. Commun.* **12**, 1–12 (2021).
96. Vernon, R. B. & Helene Sage, E. Contraction of fibrillar type I collagen by endothelial cells: A study in vitro. *J. Cell. Biochem.* **60**, 185–197 (1996).
97. Davis, G. E. & Senger, D. R. Endothelial extracellular matrix: Biosynthesis, remodeling, and functions during vascular morphogenesis and neovessel stabilization. *Circ. Res.* **97**, 1093–1107 (2005).
98. van Hinsbergh, V. W. M., Engelse, M. A. & Quax, P. H. A. Pericellular proteases in angiogenesis and vasculogenesis. *Arterioscler. Thromb. Vasc. Biol.* **26**, 716–728 (2006).

99. Veidal, S. S. *et al.* Assessment of proteolytic degradation of the basement membrane: A fragment of type IV collagen as a biochemical marker for liver fibrosis. *Fibrogenes. Tissue Repair* **4**, 22 (2011).
100. Sand, J. M. *et al.* MMP mediated degradation of type IV collagen alpha 1 and alpha 3 chains reflects basement membrane remodeling in experimental and clinical fibrosis - Validation of two novel biomarker assays. *PLoS ONE* **8**, 84934 (2013).
101. Wang, J. *et al.* Cathepsin G deficiency reduces periaortic calcium chloride injury-induced abdominal aortic aneurysms in mice. *J. Vasc. Surg.* **62**, 1615–1624 (2015).
102. Kafienah, W., Buhle, D. J., Burnett, D. & Hollander, A. P. Cleavage of native type I collagen by human neutrophil elastase. *Biochem. J.* **330**, 897–902 (1998).
103. Håkanson, M., Textor, M. & Charnley, M. Engineered 3D environments to elucidate the effect of environmental parameters on drug response in cancer. *Integr. Biol.* **3**, 31–38 (2011).
104. Edmondson, R., Adcock, A. F. & Yang, L. Influence of matrices on 3D-cultured prostate cancer cells' drug response and expression of drug-action associated proteins. *PLoS ONE* **11**, e0158116 (2016).
105. Lampi, M. C. & Reinhart-King, C. A. Targeting extracellular matrix stiffness to attenuate disease: From molecular mechanisms to clinical trials. *Sci. Transl. Med.* **10**, 475 (2018).
106. Nakasaki, M. *et al.* The matrix protein Fibulin-5 is at the interface of tissue stiffness and inflammation in fibrosis. *Nat. Commun.* **6**, 8574 (2015).
107. Shen, Y. *et al.* Reduction of liver metastasis stiffness improves response to bevacizumab in metastatic colorectal cancer. *Cancer Cell* **37**, 800–817.e7 (2020).
108. Schindelin, J. *et al.* Fiji: An open-source platform for biological-image analysis. *Nat. Methods* **9**, 676–682 (2012).
109. Schmid, B., Schindelin, J., Cardona, A., Longair, M. & Heisenberg, M. A high-level 3D visualization API for Java and ImageJ. *BMC Bioinform.* **11**, 274 (2010).

Author contributions

R.R. designed, performed and analysed experiments and drafted the manuscript. K.J., K.H. supervised research direction and edited the manuscript. M.H. supervised research direction, designed experiments, and edited the manuscript.

Funding

This work was supported by an AstraZeneca-Cambridge PhD Studentship. Research in MTH lab is also supported by NC3Rs/BHF PhD studentship NC/N002350/1 and British Heart Foundation project Grant PG/20/12/34982.

Competing interests

The authors declare no competing interests.

Additional information

Supplementary Information The online version contains supplementary material available at <https://doi.org/10.1038/s41598-022-10849-x>.

Correspondence and requests for materials should be addressed to M.T.H.

Reprints and permissions information is available at www.nature.com/reprints.

Publisher's note Springer Nature remains neutral with regard to jurisdictional claims in published maps and institutional affiliations.



Open Access This article is licensed under a Creative Commons Attribution 4.0 International License, which permits use, sharing, adaptation, distribution and reproduction in any medium or format, as long as you give appropriate credit to the original author(s) and the source, provide a link to the Creative Commons licence, and indicate if changes were made. The images or other third party material in this article are included in the article's Creative Commons licence, unless indicated otherwise in a credit line to the material. If material is not included in the article's Creative Commons licence and your intended use is not permitted by statutory regulation or exceeds the permitted use, you will need to obtain permission directly from the copyright holder. To view a copy of this licence, visit <http://creativecommons.org/licenses/by/4.0/>.

© The Author(s) 2022